Available online at www.sciencedirect.com
SCIENCE DIRECT
ELSEVIER
Ocean Engineering 33 (2006) 168–180
OCEAN ENGINEERING
www.elsevier.com/locate/oceaneng

A novel technique in analyzing non-linear wave-wave interaction

Mohamed A.K. Elsayed*

Department of Engineering Science and Mechanics, Virginia Polytechnic Institute and State University, P. O. Box 0219, Blacksburg, VA 24061, USA

Received 2 November 2004; accepted 13 April 2005
Available online 20 July 2005

Abstract

During wave growth non-linear wave–wave interactions cause transfer of some wave energy from lower to higher wave periods as the spectrum grows. Wavelet bicoherence, which is a new technique in the analysis of wind–wave and wave–wave interactions, is used to analyze non-linear wave–wave interactions. A selected record of wind wave that contains the maximum wave height observed during 6 h of wave generation is divided into five segments and wavelet bicoherence is computed for the whole record, and for all divided segments. The study shows that the non-linear wave–wave interaction occurs at different bicoherence levels and these levels are different from one segment to another due to the non-stationarity feature of the examined data set.

Keywords: Morlet wavelet; Cross-spectrum; Cross-bispectrum; Wave growth; Phase coupling

1. Introduction

Wave growth is considered one of the most complex phenomenon in the field of coastal engineering. Several studies have been carried out over a century to analyze wave generation by wind and wave growth in attempt to understand these mechanisms. Among those studies are; (Phillips, 1957, 1958; Miles, 1957, 1959a,b, 1962, 1967; Lighthill, 1962; Kraus and Businger, 1994; Donelan and Hui, 1990).

* Fax: +1 540 231 4574.
E-mail address: melsayed@vt.edu.

0029-8018/$ - see front matter © 2005 Elsevier Ltd. All rights reserved.
doi:10.1016/j.oceaneng.2005.04.010

One of the important phenomenons associated with wave growth is a non-linear wave–wave interaction because this interaction causes transfer of some wave energy from lower to higher wave periods as the spectrum grows.

This article aims at analyzing the non-linear wave–wave interaction during wave growth in a Mistral event by using wavelet bicoherence, which is a new tool in the analysis of wind–wave and wave–wave interactions.

The wavelet bicoherence is a measure of phase coupling that occurs in a signal or between two signals. Phase coupling is defined to occur when two frequencies, $f1, f2$, are simultaneously present in the signal(s) along with their sum (or difference) frequencies, and the sum of the phases of these frequency components remains constant. The bicoherence measures this quantity and is a function of two frequencies $f1$ and $f2$ which is close to 1 when the signal contains three frequencies $f1, f2, f$ that satisfy the relation $f=f1+f2$; if this relation is not satisfied, it is close to zero (Milligen et al., 1995).

2. Collected data

The data used in this work was collected during FETCH experiment (Drennan et al., 2003). An ASIS buoy was deployed on 18th March, 1998, and remained until 10th April, 1998. This period corresponds to Mistral event, which is a regional wind occurring during the conditions of high pressure over western Europe/Bay of Biscay, combined with a low pressure system south of the Alps. The Mistral is characterized by a strong, steady and cold flow with near surface wind speeds frequently in excess of 30 m/s (Drennan et al., 2003). The selected record contains the maximum wave height observed during six hours of wave generation. The length of the record is 1706 s of continuous measured wave height (Fig. 1). The record is divided sequentially into five segments each one has a length of 341 sec as shown in Figs. 2–6, respectively.

3. Analysis method

3.1. Continuous wavelet analysis

The continuous wavelet transform $W(a,\tau)$ of a function h(t), is defined as:

$$W(a,\tau) = \int_{-\infty}^{+\infty} h(t)\psi^*(t)\mathrm{d}t \tag{1}$$

where a and τ are scale and time variables respectively, and $\psi_{a\tau}$ represents the wavelet family generated by continuous translations and dilations of the mother wavelet $\psi(t)$. These translations and dilations are obtained by

$$\psi_{a,\tau} = \frac{1}{\sqrt{a}}\psi\left(\frac{t-\tau}{a}\right) \tag{2}$$

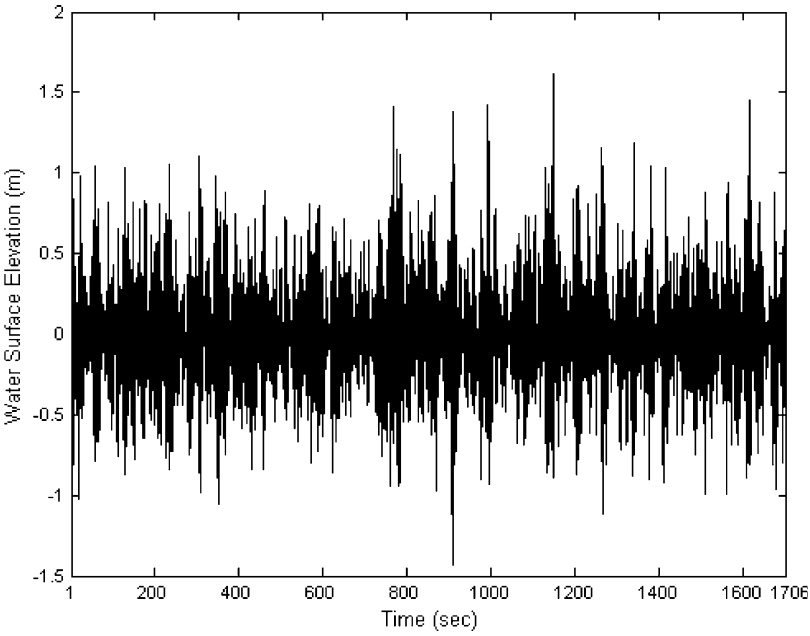

Fig. 1. Time Series of wind-wave (whole record).

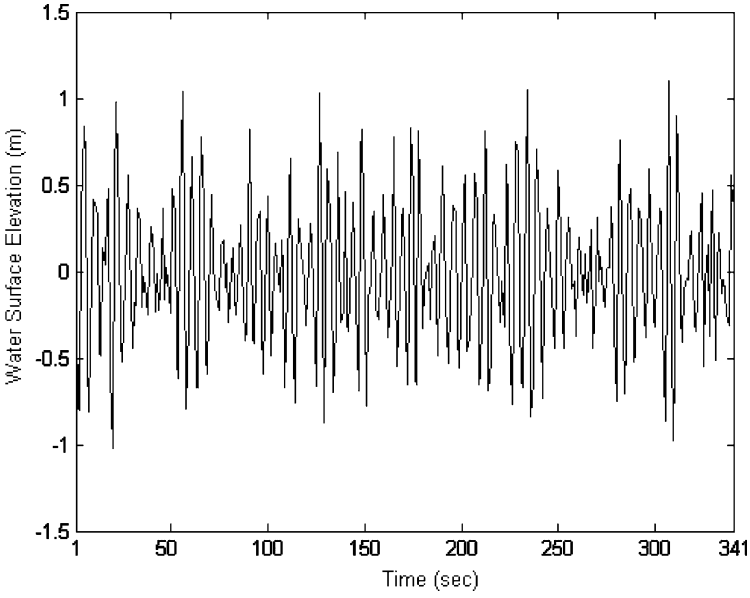

Fig. 2. Time Series of wind-wave (segment one).

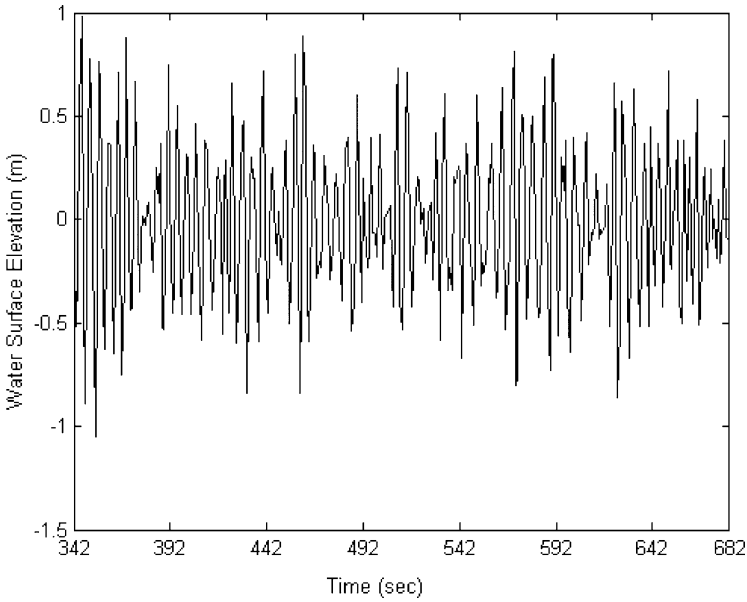

Fig. 3. Time series of wind-wave (segment two).

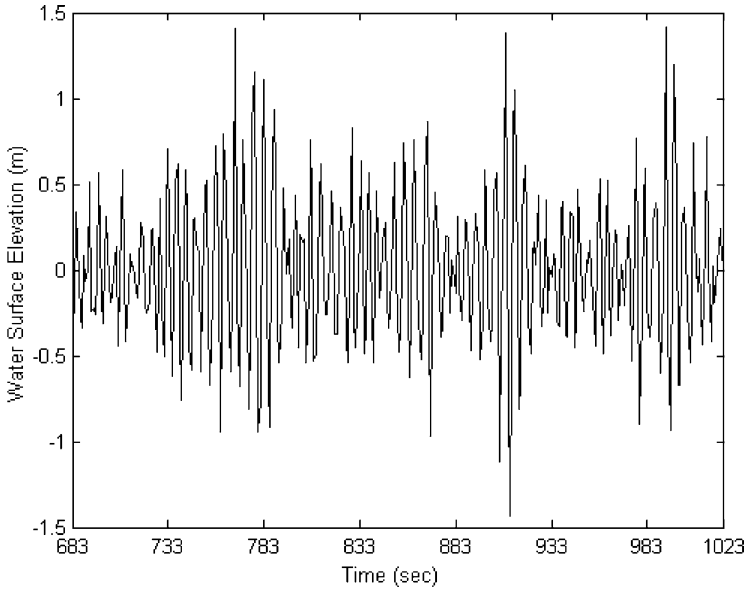

Fig. 4. Time series of wind-wave (segment three).

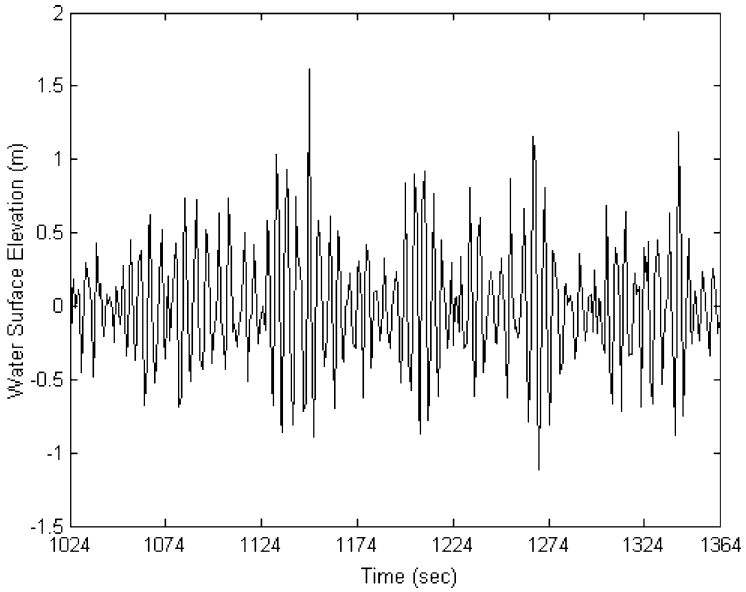

Fig. 5. Time series of wind-wave (segment four).

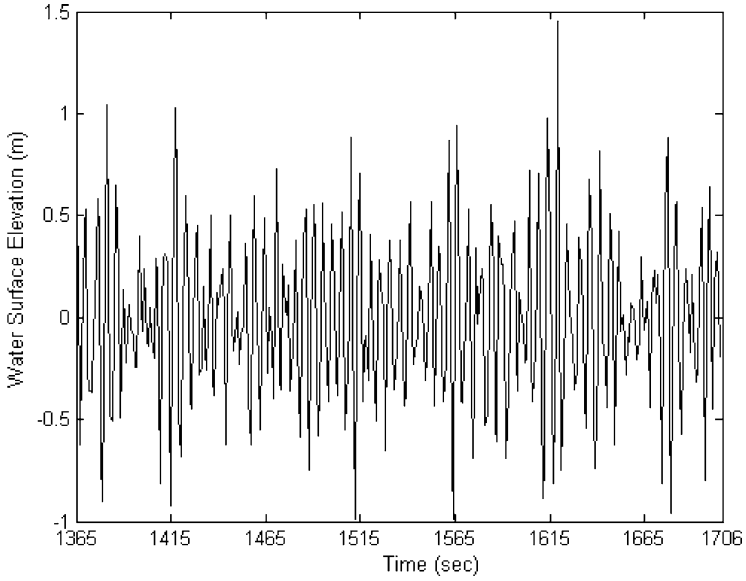

Fig. 6. Time series of wind-wave (segment five).

Following Torrence and Compo (1998); Addison (2002), the complex Morlet wavelet (Morlet, 1981) to be implemented in this study is defined as:

$$\psi(t) = \Pi^{-1/4} e^{iw_o t} e^{\frac{-t^2}{2}} \tag{3}$$

In this definition, w_o is chosen to be 6.0 to approximately satisfy the wavelet admissibility condition (Farge, 1992).

Torrence and Compo (1998) developed a code for computing the continuous wavelet transform of the time series of the signal. In this work the code was modified to compute the cross-bispectrum and the wavelet cross-bicoherence.

3.2. Power-spectrum

In order to have a statistical stability the wavelet power spectrum is integrated over a finite time interval (Milligen et al., 1995, 1997). The wavelet power spectrum:

$$P_{xx} = \int_T W_x^*(a,\tau) W_x(a,\tau) \mathrm{d}\tau \tag{4}$$

$W_x(a,\tau)$: wavelet transform of the time series
$W_x(a,\tau)$: the complex conjugate of wavelet transform of the time series
T: a finite time interval

3.3. Cross-spectrum

The wavelet cross-spectrum is defined as follows:

$$P_{xy} = \int_T W_x^*(a,\tau) W_y(a,\tau) \mathrm{d}\tau \tag{5}$$

$W_x(a,\tau)$ the complex conjugate of wavelet transform of the first time series
$W_y(a,\tau)$ the wavelet transform of the second time series

It should be noted that the results of the cross-spectrum depends heavily on the fluctuations of the individual signals because if one of the signals is fluctuated less than the other the effect of the more fluctuating signal will dominate in the resultant cross-spectrum (Hajj et al., 1998).

3.4. Linear-coherence

The normalized wavelet cross-spectrum (to have values between 0 and 1) gives the linear coherence as follows:

$$Coh_{xy}(a) = \frac{|P_{xy}(a)|^2}{P_{xx}(a)P_{yy}(a)} \tag{6}$$

$Coh_{xy}(a)$ linear coherence between two time series
$P_{xx}(a)$ power spectrum of first time series
$P_{yy}(a)$ power spectrum of second time series
$P_{xy}(a)$ cross-spectrum of the first and the second time series

3.5. Cross-bispectrum

The wavelet cross-bispectrum is defined as follows:

$$B_{yxx}(a1, a2) = \int_T W_y^*(a, \tau) W_x(a1, \tau) W_x(a2, \tau) d\tau \tag{7}$$

where $\frac{1}{a} = \frac{1}{a1} + \frac{1}{a2}$ (frequency sum rule). The wavelet cross-bispectrum measures the amount of phase coupling in the time interval T, that occurs between wavelet components of scale lengths $a1$ and $a2$ of $x(t)$ and wavelet component a of $y(t)$ such that the sum rule is satisfied (Milligen et al., 1995).

3.6. Cross-bicoherence

The normalized squared wavelet cross-bicoherence is defined as:

$$[b_{yxx}(a1, a2)]^2 = \frac{|B_{yxx}(a1, a2)|^2}{\left[\int_T |W_x(a1, \tau) W_x(a2, \tau)|^2 d\tau\right]\left[\int_T |W_y(a, \tau)|^2 d\tau\right]} \tag{8}$$

3.7. Test of non-stationarity

Liu (2000) introduced an index, which can distinguish stationary signal from non-stationary signal using wavelet spectrum of the wind waves as follows:

$$N\text{index} = \sum_k \sum_l \left[\frac{W(f_k, t_l) - \psi(f_k)}{\psi(f_k)}\right]^2 \tag{9}$$

where Nindex is the Non-stationarity index, which is a positive number and the time series with high Non-stationarity index is most likely to be non-stationary. $W(f_k,t_l)$ is wavelet spectrum of the time series, $\psi(f_k)$ is obtained by integrating the wavelet spectrum with respect to time.

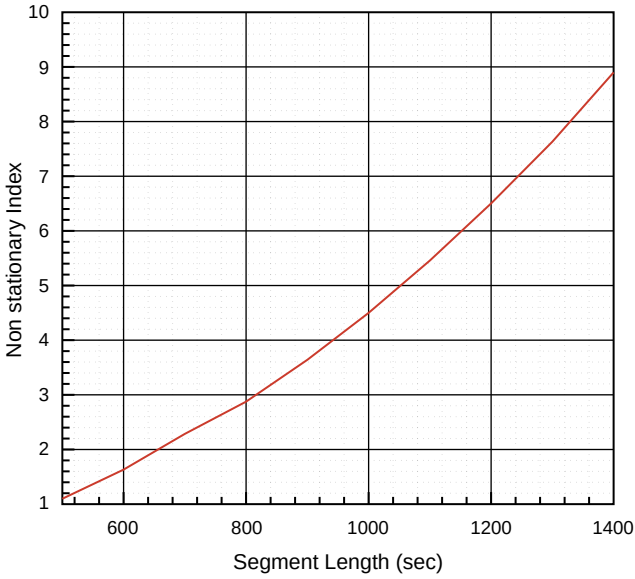

Fig. 7. Non-stationarity index for different segments of the measured wind–wave time series.

4. Results and discussions

The non-stationary test of the wind waves record is conducted by dividing the record into segments with different lengths and Eq. (9) is used to compute the nonstationarity

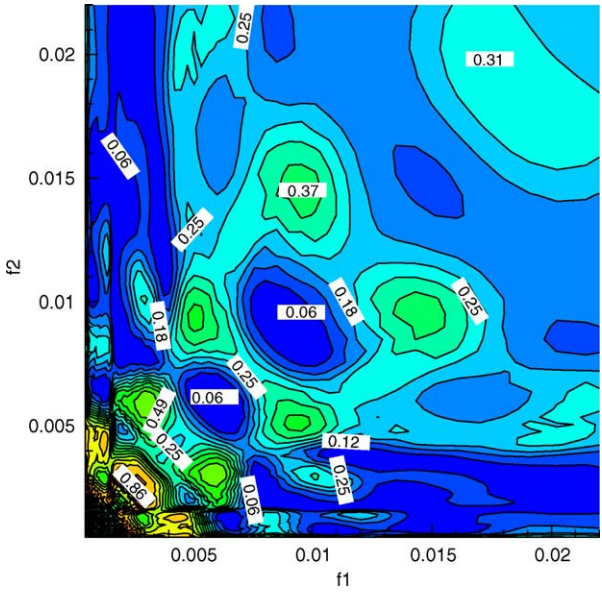

Fig. 8. Wavelet bicoherence (wave & wave & wave) for the whole record given in Fig. 1.

index for each segment. Fig. 7 gives the plot of nonstatioarity index versus segment length. The non-stationary feature of wind waves time series is clearly indicated, as there is an increase in nonstatioarity index with increasing the segment length. Therefore, the time series of wind waves is not a realization of the Gaussian random process, which agrees with Liu (2000) findings.

Wavelet bicoherence (wave & wave & wave) is computed first for the whole record of the measured wind–wave given in Fig. 1. The integration is conducted over the time ranges between 1 and 1706 s (the whole window), and the resulting wavelet bicoherence is shown in Fig. 8. The high value of wavelet bicoherence is observed at $f1$ & $f2$ range from 0.002 to 0.004.

In order to analyze the non-stationary feature of the measured record of wind–wave, the record is divided into five segments. The wavelet bicoherence (wave & wave & wave) is computed for the five segments given in Figs. 2–6, respectively. The integration for each segment is conducted over the whole window of each segment and the results are given in Figs. 9–13.

Fig. 9 shows that the high value regions of wavelet bicoherence for segment one is occurring for frequencies ranging from 0.02 to 0.005 for both $f1$ & $f2$. Also, there is a zone of high wavelet bicoherence for $f1$& $f2$ range from 0.006 to 0.008. For segment two there is a phase coupling occur at $f1$ ranges from 0.001 to 0.005 and $f1$ equals to 0.007 and 0.016 and over the same ranges for $f2$ (Fig. 10).

Figs. 11–13 give the computed wavelet bicoherence for segments three, four, and five, respectively. These plots show that non-linear wave–wave interaction and phase coupling is occurred over different ranges of frequencies and this range is different from one segment to another. This strengthens the fact that the wind wave records have

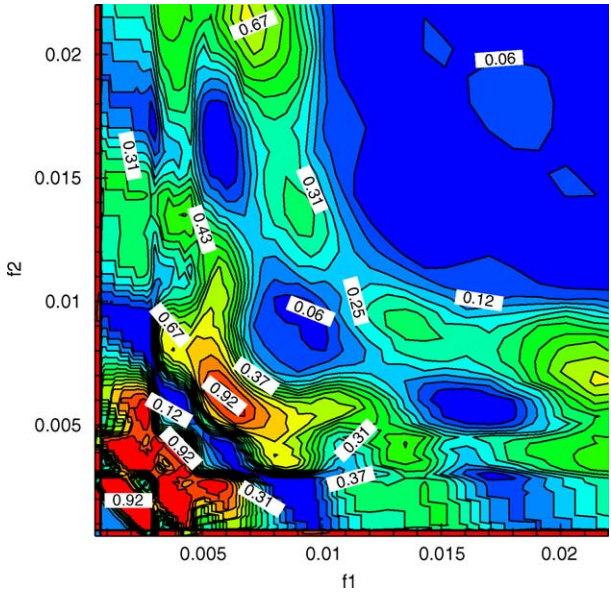

Fig. 9. Wavelet bicoherence (wave & wave & wave) for segment one.

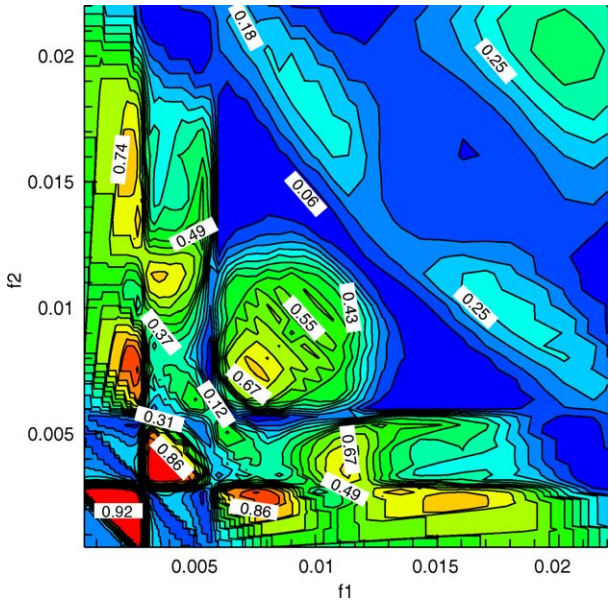

Fig. 10. Wavelet bicoherence (wave & wave & wave) for segment two.

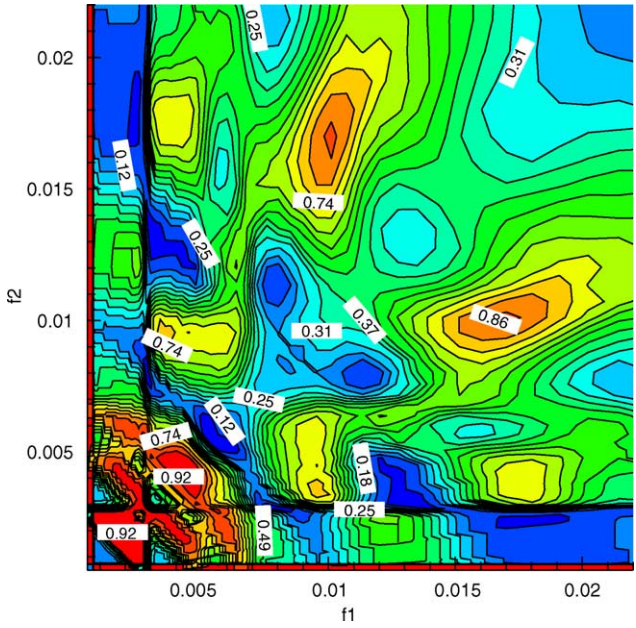

Fig. 11. Wavelet bicoherence (wave & wave & wave) for segment three.

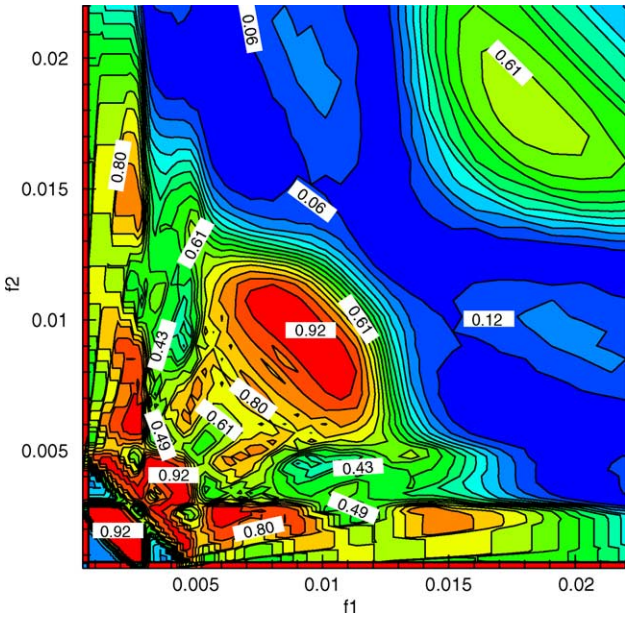

Fig. 12. Wavelet bicoherence (wave & wave & wave) for segment four.

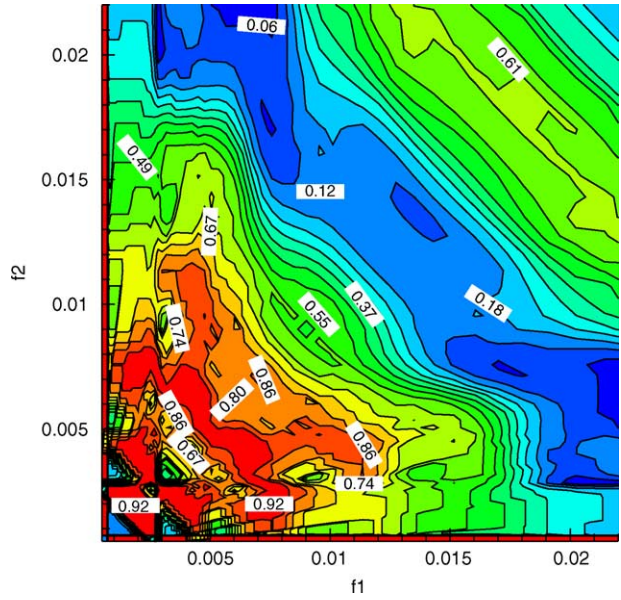

Fig. 13. Wavelet bicoherence (wave & wave & wave) for segment five.

non-stationarity feature (Liu, 2000) and hence the use of wavelet-based bicoherence deemed necessary in order to investigate the non-linear wave–wave interaction that occurs during wave growth.

The plots of wavelet bicoherence show that averaging over time for the whole record in computing wavelet bicoherence causes loss of some temporal characteristics of the signal. On the other hand, averaging over time for each segment shows that the phase coupling occurs over certain range of frequencies, which is found to be different from one segment to another. Furthermore, the results obtained in the present study show that the use of wavelet analysis with time resolution adds valuable information through the use of wavelet bicoherence in detecting the phase coupling and non-linear interaction between waves of different periods during wave growth.

5. Conclusions

During wave growth non-linear wave–wave interactions cause transfer some wave energy from lower to higher wave periods as the spectrum grows. In this study wavelet bicoherence, which is a new technique in the analysis of wind–wave and wave–wave interactions, is used to analyze non-linear wave–wave interactions and phase coupling taking place in the wave–wave interactions.

The details of wave–wave interaction during wave growth are examined by computing wavelet bicoherence for a selected record of wind–wave measurements and for the divided segments. Averaging over time for the whole record in computing wavelet bicoherence causes loss of some temporal characteristics of the signal. On the other hand, averaging over time for each segment shows that the phase coupling occurs over certain range of frequencies, and this range is found to be different from one segment to another due to the non-stationary feature of the data set.

This study adds a useful application of wavelet analysis and bispectrum analysis in detecting the phase coupling and non-linear wave–wave interaction during wave growth. Finally, it worth mentioned that the results of this study through the use of wavelet analysis could not be obtained by using the classical Fourier analysis due to the non-stationary feature that characterizes the wind–wave data set.

Acknowledgements

The author would like to thank Dr William Drennan from the Rosenstiel School of Marine and Atmospheric Science, University of Miami, Florida for providing the data necessary for conducting the present study.

References

Addison, P.S., 2002. The Illustrated Wavelet Transform Handbook, Introductory Theory and Applications in Science. Institute of Physics Publishing, Bristol, UK p. 349.

Donelan, M.A., Hui, W.H., 1990. Mechanics of ocean surface waves. In: Geernaert, G., Plant, W. (Eds.), Surface Waves and Fluxes. Kluwer Academic Publishers, The Netherlands, p. 336p.

Drennan, W.M., Graber, H.C., Hauser, D., Quentin, C., 2003. On the wave age dependence of wind stress over pure wind seas. Journal of Geophysical Research 108 (C3), 8062–8075.

Farge, M., 1992. Wavelet transforms and their application to turbulence. Annual Review of Fluid Mechanics 24, 395–457.

Hajj, M.R., Jordan, D.A., Tieleman, H.W., 1998. Analysis of atmospheric wind and pressures on a low rise building. Journal of Fluids and Structures 12, 537–547.

Kraus, E.B., Businger, J.A., 1994. Surface Wind Waves. Atmosphere and Ocean International. Oxford University Press, New York p. 362.

Lighthill, M.J., 1962. Physical interpretation of the mathematical theory of wave generation by wind. Journal of Fluid Mechanics 14, 385–398.

Liu, P.C., 2000. Is the wind wave frequency spectrum outdated. Ocean Engineering 27, 577–588.

Milligen, B.P.V., Sanchez, E., Estrada, T., Hidalgo, C., Branas, B., Carrersa, B., Garcia, L., 1995. Wavelet bicoherence: a new turbulence analysis tool. Physics of Plasma 2 (8), 3017–3032.

Milligen, B.P.V., Hidalgo, C., Sanchez, E., Pedrosa, M.A., Balbin, R., Garcia-Cortes, I., Tynan, G.R., 1997. Statistically robust linear and nonlinear wavelet analysis applied to plasma edge turbulence. Review of Scientific Instruments 68 (1), 967–970.

Miles, J., 1957. On the generation of surface waves by shear flows. Journal of Fluid Mechanics 3, 185–204.

Miles, J., 1959a. On the generation of surface waves by shear flows. Part 2. Journal of Fluid Mechanics 6, 568–582.

Miles, J., 1959b. On the generation of surface waves by shear flows. Part 3: Kelvin-Helmholtz instability. Journal of Fluid Mechanics 6, 583–598.

Miles, J., 1962. On the generation of surface waves by shear flows. Part 4. Journal of Fluid Mechanics 13, 433–448.

Miles, J., 1967. On the generation of surface waves by shear flows. Part 5. Journal of Fluid Mechanics 30, 163–175.

Morlet, J., 1981. Sampling theory and wave propagation, Proceedings of the51st Annual Meeting of the Society Exploration Geophysics, Los Angeles, USA 1981.

Phillips, O.M., 1957. On the generation of waves by turbulent wind. Journal of Fluid Mechanics 2, 417–445.

Phillips, O.M., 1958. The equilibrium range in the spectrum of wind-generated waves. Journal of Fluid Mechanics 4, 426–434.

Torrence, C., Compo, G.P., 1998. A practical guide to wavelet analysis. Bulletin of the American Meteorology Society 79 (1), 61–77.